Published in final edited form as:
Cell Rep. 2014 December 24; 9(6): 2071–2083. doi:10.1016/j.celrep.2014.11.021.

Hand2 is an Essential Regulator for Two Notch-Dependent Functions within the Embryonic Endocardium

Nathan J. VanDusen, Ph.D.[1], **Jose Casanovas**[1], **Joshua W. Vincentz, Ph.D.**[1], **Beth A. Firulli**[1], **Marco Osterwalder**[2], **Javier Lopez-Rios**[2], **Rolf Zeller**[2], **Bin Zhou**[3], **Joaquim Grego-Bessa**[4], **José Luis De La Pompa**[5], **Weinian Shou**[1], and **Anthony B. Firulli**[1,*]

[1]Riley Heart Research Center, Wells Center for Pediatric Research, Departments of Pediatrics and Medical and Molecular Genetics, Indiana University, Indianapolis, IN 46202, USA [2]Developmental Genetics, Department of Biomedicine, University of Basel, CH-4058 Basel, Switzerland [3]Department of Genetics, Albert Einstein College of Medicine, New York, NY 10461, USA [4]Department of Developmental Biology, Memorial Sloan Kettering Cancer Center, New York, NY 10021, USA [5]Cardiovascular Developmental Biology Program, Cardiovascular Development and Repair Department, Centro Nacional de Investigaciones Cardiovasculares (CNIC), Madrid, 28029, Spain

Summary

The bHLH transcription factor Hand2 plays critical roles during cardiac morphogenesis via expression and function within myocardial, neural crest, and epicardial cell populations. Here we show that Hand2 plays two essential Notch-dependent roles within the endocardium. Endocardial ablation of *Hand2* results in failure to develop a patent tricuspid valve, intraventricular septum defects, and hypotrabeculated ventricles, which collectively resemble the human congenital defect tricuspid atresia. We show endocardial Hand2 to be an integral downstream component of a Notch endocardium-to-myocardium signaling pathway, and a direct transcriptional regulator of *Neuregulin1*. Additionally, Hand2 participates in endocardiumto-endocardium based cell-signaling, with *Hand2* mutant hearts displaying an increased density of coronary lumens. Molecular analyses further reveal dysregulation of several crucial components of Vegf signaling, including *VegfA*, *VegfR2*, *Nrp1*, and *VegfR3*. Thus, Hand2 functions as a crucial downstream transcriptional effector of endocardial Notch signaling during both cardiogenesis and coronary vasculogenesis.

*Corresponding Author Anthony B. Firulli Indiana University Riley Heart Research Center Indianapolis, UNITED STATES Fax: 317-278-5413 tfirulli@iu.edu.

Author Contributions NJV wrote manuscript, conceived of experiments, and carried out experiments. JC carried out experiments and critically read manuscript. JWV and BAF interpreted data, provided reagents, and critically read manuscript. RZ, MO, and JLR conceived of and carried out *Hand2-3xFLAG* Chip-seq. BZ aided in experimental planning and provided *Nfatc1*^{Cre} mice. JGB and JLP assayed *Hand2* expression in RBPJk$^{-/-}$ mice. WS interpreted data and evaluated manuscript. ABF wrote and edited manuscript and conceived of experiments.

Keywords

Hand2; Nrg1; EfnB2; Tricuspid atresia; endocardium; Notch signaling

Introduction

In the primitive heart, communication between the endocardium, which is the endothelium-like tissue that lines the heart, and the myocardium, which is the muscular heart tissue, is essential for processes central to normal cardiac morphogenesis, including trabeculation, chamber septation, and coronary vasculogenesis (Bruneau, 2003; Brutsaert, 2003). The transmembrane receptor Notch1 is integral to this communication, as endocardial Notch activates endocardial EphrinB2, which through-unknown mechanisms, activates expression of the secreted factor Neurgulin1 (*Nrg1*). Nrg1 initiates the trabeculation process, and Notch signaling subsequently activates expression of Bmp10 (Chen et al., 2004) through a separate pathway (Grego-Bessa et al., 2007). Bmp10 expression stimulates proper proliferation of trabecular, and possibly septal, myocardium. Disruption of Notch-mediated endocardialmyocardial communication results in congenital heart defects (CHD), which are the most frequent human developmental anomalies (Hoffman, 1995).

Tricuspid atresia (TA) is a CHD characterized by the lack of a direct connection between the right atria (RA) and the right ventricle (RV), requiring both ventricular (VSD) and atrial (ASD) septal defects for embryonic survival (Anderson et al.). Conditional ablation of the bHLH factor *Hand2* within the second heart field (SHF) via *Mef2c-Cre* results in TA (Tsuchihashi et al., 2011). *Mef2c-Cre* marks a pool of SHF progenitor cells that contribute to both the myocardium and endocardium (Tsuchihashi et al., 2011; Verzi et al., 2005), and SHF ablation of Hand2 causes TA via unknown mechanisms. As cardiomyocyte-specific ablation of *Hand2* does not result in TA (Tsuchihashi et al., 2011), we hypothesized that loss of Hand2 function within the endocardium is causative of TA. Indeed, our data reveals that either endothelial or endocardial-specific deletion of *Hand2* (*H2CKO*) using either *Tie2-Cre* or $Nfatc1^{Cre}$, respectively, results in TA. These data show that Hand2 functions downstream of endocardial Notch to mediate endocardium-to-myocardium signaling via direct transcriptional regulation of the growth factor *Neuregulin1* (*Nrg1*).

As cardiogenesis proceeds, development of the coronary vasculature allows for oxygenation of the thickening ventricular compact zone. Cardiac endothelial cells form the primitive coronary network by angiogenesis (Red-Horse et al., 2010; Wu et al., 2012), a process that extra-cardiac models demonstrate to be Notch-dependent. Early embryonic lethality in Notch pathway mutants has precluded robust analysis of Notch signaling in coronary development. Significantly, *H2CKO* mice survive long enough to assess the initiation of coronary vascularization, and our findings indicate that Hand2 modulates coronary development through regulation of multiple Vegf signaling components within the developing heart. Collectively, these data support a model whereby Notch signaling, via endocardial Hand2 function, regulates trabeculation, interventricular septum (IVS) formation, and coronary development.

Results

Endothelial/endocardial loss of Hand2 causes trabeculation and septation defects that resemble tricuspid atresia

To test the hypothesis that loss of endocardial *Hand2* results in TA, we intercrossed the endothelial cell-specific *Tie2-Cre* allele (Kisanuki et al., 2001) with mice carrying the *Hand2* conditional allele (*Hand2*^{fx}). *Tie2-Cre* is expressed in all endothelial cells, including cells of the ventricular endocardium, coronary endothelium, and atrioventricular cushions (Kisanuki et al., 2001). *Tie2-Cre* expression initiates at E8.5 (Kisanuki et al., 2001), which is concurrent with the onset of endocardial *Hand2* expression (Barnes et al., 2011). *Hand2*$^{fx/fx}$;*R26R*^{lacZ} females were mated with *Tie2-Cre(+);Hand2*$^{+/-}$ males, and neonates were genotyped. No *H2CKO* mice were observed (n=58, Table S1). We next set up timed matings and observed that *Tie2-Cre(+);Hand2*$^{fx/-}$ embryos die by E14.5 (Table S1). *Hand2* deletion within the endocardium is evident by *in situ* hybridization (*ISH*) at E10.5 (Fig. 1A, B arrows). Examination of *Tie2-Cre H2CKOs* in whole mount (Fig. 1D, E) and in section histology (Fig. 1G, H) reveals hypotrabeculation (arrow in E) and a highly penetrant TA phenotype (Fig. 1H; Table S2) comparable to that reported in the SHF *Mef2c-CreH2CKOs*. At E12.5, we observe hypotrabeculation, VSDs, rightward septal displacement, and RV hypoplasticity in *Tie2-Cre H2CKO* hearts. Occasionally (~20%), we observe a patent tricuspid valve that makes a direct connection with the LV, resulting in a double inlet left ventricle (DILV), a CHD that functionally resembles TA (Fig. 1J arrow).

To examine atrioventricular (AV) cushion formation, cell density, and extracellular matrix (ECM) deposition, we stained sections with alcian blue. Although comparison of *H2CKO* cushions with those of controls revealed no difference in size, (Fig 1K, L), there appears to be a cushion-positioning defect (asterisk in Fig. 1L). Despite normal AV cushion ECM deposition, no direct connection between the RA and RV is detected in any plane of section, resulting in a single left sided AV canal in most *H2CKOs*, thus meeting the clinical definition of TA (Fig. 1H). However, OFT morphogenesis occurs normally in *H2CKOs* (Fig. S1A–C).

While we also observe no defects in the yolk sac vasculature of *Tie2-CreH2CKOs* (Fig. S1D, E), Hand2 may play critical roles in vascular endothelium that could contribute to the observed embryonic lethality. Therefore, we used the endocardial-specific *Nfatc1*^{Cre} allele (Wu et al., 2012) to generate *H2CKOs* (Fig. 1C, F, N). This *Nfatc1*^{Cre} allele initiates expression throughout the endocardium at E9.0 (Wu et al., 2012), as opposed to the *Nfatc1*^{enCre} allele, which labels only a subset of valve endothelial cells. *Nfatc1*^{Cre} *H2CKOs* also show dramatic defects in trabeculation, malformed IVS, and atresia of the tricuspid valve (~70%; Fig. 1F, N). Interestingly, in some cases, IVS malformations include large protrusions of myocardium that appear to indicate the formation of multiple IVSs (Fig. 1N arrows; Table S2). Robust expression of the septal/compact zone marker *Hey2* and the septal marker *Irx2* in these large protrusions confirm this observation, while expression of the trabecular marker Anf is excluded (Fig. S2A–H). However, expression of the LV marker *Hand1* is not observed beyond the left-most septum (Fig. S2I, J). Tbx5, which has been suggested to induce the IVS (Takeuchi et al., 2003), is also unchanged (Fig. S2K, L).

Together, these data confirm that conditional deletion of *Hand2* within the endocardium is critical for normal trabeculation and septation. Given that these phenotypes are myocardial in nature, this suggests that endocardial Hand2 plays a crucial role in endocardium-to-myocardium signaling.

Hand2 regulates *Nrg1* expression within the endocardium

We next investigated changes in gene expression within E10.5 *Tie2-CreH2CKOs* using *ISH*. Expression analysis of *Fog2* was of interest, as *Fog2* deficient mice also display TA (Svensson et al., 2000); however, no change in *Fog2* expression was observed (Fig. S3A, B). Deletion of *Tgfbr2* from the endothelium results in DILV (Jiao et al., 2006). Analysis of *Tgfbr2* expression revealed no differences between *H2CKO* and controls (Fig. S3C, D).

It has been directly demonstrated that endocardial Notch signaling plays an essential role in orchestrating morphogenic changes within the underlying myocardium, particularly during the process of trabeculation (Grego-Bessa et al., 2007). Therefore, we examined Notch pathway gene expression. We first analyzed expression of the Notch-regulated bHLH transcriptional repressors, and potential Hand2 dimer partners, *Hey1* and *Hey2* (Fig. S3E–H). Endocardial expression is not significantly changed. Next, we examined expression of the direct Notch1 target *EphrinB2* (*EfnB2*; Grego-Bessa et al., 2007). *EfnB2* ISH also shows no change in expression between *H2CKOs* and control embryos (Fig. 2A–D). However, EGF family member *Neuregulin1* (*Nrg1*) is markedly down-regulated at E10.5 within the endocardium of *H2CKOs* (Fig. 2F, arrow H) compared to control embryos (Fig. 2E, arrow G). *Nrg1* is known to be an essential mediator of trabeculation in the developing ventricles and is down-regulated in *Tie2-Cre Notch1*CKOs, and *EfnB2* systemic null embryos (Grego-Bessa et al., 2007). The maintenance of *EfnB2* and loss of *Nrg1* in *H2CKOs* suggests that Hand2 acts downstream of *EfnB2*, but upstream of *Nrg1*, representing a novel step in *Notch1* trabeculation and septation signaling.

We next analyzed *Bmp10* expression, as myocardially-expressed Bmp10 is crucial for proper trabeculation and is independently downstream of Notch1 signaling (Chen et al., 2004; Grego-Bessa et al., 2007). *BMP10* ISH at E10.5 suggests a subtle down-regulation in *H2CKOs* (Fig. S3I, J) while E12.5 ISH shows a near complete loss of *Bmp10* expressing trabecular tissue within the RV but not LV (Fig. 2I, J arrows). To quantitatively assess *Bmp10* expression, we dissected ventricles from E10.5 hearts, and isolated RNA for qRT-PCR (qPCR). As expected, qPCR analysis confirms that both *Hand2* and *Nrg1* are significantly down-regulated in *H2CKOs* (Fig. 2K) but *Bmp10* myocardial expression is not altered (Fig. 2K). Thus, the reduction of *Bmp10* within the RV of E12.5 *H2CKOs* reflects the absence of RV trabeculation, as LV trabeculae express *Bmp10* (Fig. 2J).

Endocardial Hand2 functions downstream of Notch1 and the direct Notch1 target EfnB2

Upon interaction with one of its transmembrane ligands, the transmembrane receptor Notch1 is proteolytically cleaved to generate the Notch1 intracellular domain (N1ICD). N1ICD translocates to the nucleus where it dimerizes with its partner RBPJk to activate transcription of target genes. Previous studies have shown that deletion of *Notch1* or *RBPJk* results in hypotrabeculation due to loss of *EfnB2* and *Nrg1* (Grego-Bessa et al., 2007). To confirm that

Hand2 lies within the *Notch1* signaling pathway, we assayed *Hand2* expression in E9.5 *RBPJk*$^{-/-}$ embryos. Whole mount analyses reveal a loss of endocardial *Hand2*, while expression within the OFT and pharyngeal mesenchyme is unaffected (Fig. 3A, B). Sectioned embryos confirm a specific loss of *Hand2* within mutant endocardium (Fig. 3C, D), definitively establishing Hand2 as a Notch1 signaling effector.

During trabeculation N1ICD/RBP Jk directly *trans*-activates *EfnB2*, which acts through its EphB2/EphB4 tyrosine kinase receptors to upregulate *Nrg1* (Grego-Bessa et al., 2007). While our data clearly show *Hand2* to be upstream of *Nrg1*, it was not clear if *Hand2* lies downstream of *EphrinB2* signaling, or if *Hand2* represents a parallel *EfnB2*-independent Notch signaling pathway. To address this question, we assayed *Hand2* expression in E9.5 *Tie2-Cre(+);EfnB2*$^{fx/fx}$ embryos (Gerety and Anderson, 2002). ISH reveals that *Hand2* is down-regulated in endocardial cells of *Tie2-Cre(+);EfnB2*$^{fx/fx}$ embryos (Fig. 3F arrow), whereas Hand2 expression in pharyngeal mesenchyme and the proepicardial organ is unaffected when compared to control hearts (Fig. 3E). qPCR analysis at E10.5 confirms *Hand2* down-regulation within *Tie2-Cre(+);EfnB2*$^{fx/fx}$ isolated ventricles (Fig. 3G). Together, these data show that Hand2 is a Notch-dependent endocardial factor positioned between *EfnB2* and *Nrg1*.

Hand2 regulation of *Nrg1* is direct via interaction with the *Nrg1* promoter and upstream enhancer sequences

As *Hand2* encodes a transcription factor with a similar expression profile to *Nrg1*, we sought to determine if Hand2 regulation of *Nrg1* is direct. An 850bp region of the *Nrg1* promoter has been identified as necessary for high *Nrg1* transcriptional activity *in vitro* (Frensing et al., 2008). As Hand2 binds the consensus sequence CANNTG, termed an E-box, or alternatively CGNNTG, a D-box (Firulli et al., 2007), we searched this aligned promoter region for these conserved *cis*-elements. Three were found within the 500bp directly upstream of the *Nrg1* translation start site (Fig. 4A). To assess Hand2 interaction with this region of the *Nrg1* promoter, we conducted ChIP assays in HeLa cells, employing a Myc-tagged Hand2 co-transfected with a plasmid encoding an untagged Hand2 dimerization partner E12. Negative controls included Myc-Hand2 + E12 immuno-precipitated without αMyc, and *pCS2+Myc* samples immuno-precipitated with αMyc. Enrichment of the *Nrg1* promoter region was assessed by PCR using primers corresponding to a 103bp region of the human *Nrg1* promoter. This amplicon shows robust enrichment within Myc-Hand2 + E12 immuno-precipitated samples (Fig. 4B). To confirm that Hand2-E12 heterodimers are capable of binding the conserved consensus E/D-box sequences, double-stranded oligos corresponding to these sites were used in electrophoretic mobility shift assays (EMSA) with *in vitro* translated Hand2 and E12 (Fig. 4C). Hand2-E12 heterodimers specifically bind oligos corresponding to sites 1 and 3 (Fig. 4D, E). No DNA binding is observed between Hand2-E12 complexes and site 2. To test if Hand2 is capable of *trans*-activating the *Nrg1* promoter, *Hand2* and *E12* expression constructs were transfected into HeLa cells along with a *Nrg1* luciferase reporter containing the 1000bp directly upstream of the murine *Nrg1* translation start site. This region contains multiple transcription start sites located between −395 and −425 (Frensing et al., 2008). Co-transfection of *Hand2* and *E12* resulted in 7-fold reporter activation. Subsequent assays

utilizing truncated promoters (−500/0bp and −500/−250bp) demonstrated more robust activation (~18 and 16 fold respectively; Fig. 4F). Transactivation data from the 500bp promoter revealed that E12 alone is not sufficient for activation, while Hand2 alone results in only modest (but significant) 3.5 fold transactivation. Consistent with EMSA results, co-transfection of Hand2 and E12 results in 18-fold transactivation, while a DNA binding deficient *Hand2* construct (Hand2Δbasic) is incapable of *Nrg1trans*-activation alone or when co-transfected with E12 (Fig. 4G).

Replacement of *Hand2* within *EfnB2* deficient endocardium results in an improvement of cardiac trabeculation

EfnB2 mutant embryos display hypotrabeculation accompanied by loss of *Hand2* and *Nrg1* expression (Fig. 4). Therefore, if Hand2 is both necessary and sufficient for regulation of *Nrg1*, we reasoned that *Hand2* replacement in *Nfatc1^{Cre} EfnB2CKOs* would restore *Nrg1* expression and improve ventricular trabeculation. To test this, we generated the Creactivatable *Hand2* transgene *CAG-CAT-Hand2* (*CC-H2*; Fig. S4A). Ectopic expression of Hand2 in limb mesenchyme results in preaxial polydactyly (McFadden et al., 2002). As predicted, *Prx1-Cre* mediated activation of *CC-H2* within the limb results in polydactyly, indicating that the conditional transgene can be efficiently and specifically activated (Fig. S4B). Similarly, *Nfatc1^{Cre}* efficiently activates *CC-H2* in the endocardium (Fig. S4C). E13.5 *Nfatc1^{Cre}*;*CC-H2(+)* embryos do not display any obvious cardiac phenotypes (data not shown). Subsequently, *CC-H2(+); EfnB2$^{fx/+}$* females were then crossed with *Nfatc1^{Cre}*; *EfnB2$^{fx/+}$* males to generate *Nfatc1^{Cre}*; *CC-H2(+); EfnB2 CKOs*. *CC-H2*(−); *EfnB2 CKOs* die by E11.5, with severe pericardial edema, hemorrhaging, and defects in cardiac looping and chamber development (Fig. 5C). These phenotypes closely resemble the defects observed in *Tie2-Cre EfnB2 CKOs* (Gerety and Anderson, 2002), indicating that while EfnB2 function within extracardiac vasculature is likely important, loss of endocardial *EfnB2* is sufficient to cause mid-gestation lethality. *Hand2* ISH at E10.5 confirms robust endocardial *Hand2* expression in controls (Fig. 5E, F), and loss of *Hand2* in *EfnB2 CKOs* (Fig. 5G arrow). The presence of the *CC-H2* allele restores *Hand2* expression within the *EfnB2 CKOs* (Fig. 5H arrow; n = 3). *Nrg1* ISH reveals robust expression in controls (Fig. 5I, J), and loss of *Nrg1* expression in *EfnB2 CKOs* (Fig. 5K arrow). *CC-H2(+); EfnB2 CKOs* display a significant increase in *Nrg1* expression (Fig. 5L, arrow), while assessment of trabeculation by *Bmp10* ISH reveals a marked improvement in *Bmp10* expressing trabecular myocardium (Fig. 5P arrow) when compared to *EfnB2 CKOs* lacking the *CC-H2* allele (Fig. 5O arrow). Expression analysis of isolated E10.5 ventricles by qPCR demonstrates that while still well below control levels, *Nrg1* expression in *EfnB2* mutants that carry the *CC-H2* allele (n = 4) is twice as high as in *EfnB2* mutants lacking the *CC-H2* allele (upregulated 112%). *Bmp10* expression is increased by 79% with obvious improvement in trabeculation (Fig. 5Q).

Notch-dependent Hand2 function also regulates coronary angiogenesis

The above analyses demonstrate that endocardial Hand2 plays a crucial role in myocardial morphogenesis. Myocardial trabeculation and compaction are intimately linked to endothelial cell behavior during development of the coronary vasculature by a complex signaling network that includes Vegf, Fgf, Tgf-β and Notch components (Smart et al., 2009).

Furthermore, early embryonic lethality in genetic models of dysfunctional Notch signaling has precluded an *in vivo* assessment of the role of Notch signaling in formation of the coronary arteries. As we have established Hand2 as an integral component of endocardial Notch signaling, and as coronary endothelium is derived at least in part from the endocardium (Wu et al., 2012), the survival of *H2CKOs* to E14.5 allows us a unique opportunity to assess Notch function in early coronary development. Analysis of hearts at E13.5, one day after initiation of intra-myocardial coronary formation (Tian et al., 2013), shows that *Nfatc1*^{Cre} *H2CKO* hearts (Fig. 6B, D arrows) exhibit an increased density of primitive coronary vessels when compared to control ventricles (Fig. 6A, C). Subsequent analyses revealed a comparable degree of hyper-vascularization in *Tie2-Cre H2CKOs* (data not shown, Table S2). To ascertain the mechanism underlying this hyper-vascularization, we analyzed genes associated with vascular development in E10.5 and E13.5 *Nfatc1*^{Cre} *H2CKO* isolated ventricles by qPCR (n = 4, Fig. 6E and F respectively). As expected, expression levels of *Hand2* and *Nrg1* are down at both time points. Analysis of vascular markers at E10.5 reveals dysregulation of select components of Vegf signaling (Fig. 6E). *VegfR2* is downregulated by 30%, and its co-receptor *Nrp1* is downregulated by 14%. *VegfD*, which encodes a VegfR3 specific ligand, is downregulated by 25%. By E13.5, expression levels of *VegfR2* and *VegfD* have recovered (Fig. 6F), whereas *Nrp1* remains downregulated. Surprisingly, expression of *VegfA*, which encodes the primary Vegf ligand that regulates vascular development (Ferrara et al., 1996), is upregulated by over 200%. Expression of *VegfR3* is upregulated by 120%, and expression of *Dll4*, which encodes a notch ligand regulated by VegfRs (Wythe et al., 2013), is upregulated by approximately 85%. Differential regulation of several additional key vascular factors was also observed at E13.5. The venous markers *CouptfII* and *EphB4* are downregulated by 21% and 24% respectively, while the arterial marker *EfnB2* is downregulated by 33%. Surprisingly, *Sox18* and *Lyve1*, which encode factors typically associated with endothelium of the lymphatic system, were upregulated by 45% and 73% respectively. To determine what cardiac cell populations were upregulating Lyve-1, we conducted Lyve-1 immunostaining at E10.5 (Fig. 6G, H) and E13.5 (Fig. 6I–N) in control and *H2CKO* hearts. Sections from E13.5 hearts were co-stained with VegfR2 to mark cardiac endothelium (see Table S3 for glossary of terminology pertaining to endothelial cell populations). E10.5 immunostaining reveals that Lyve-1 is expressed robustly within endocardium of both control and *H2CKO* hearts. In contrast, by E13.5, Lyve-1 immunostaining in control hearts is restricted to a population of peripheral cardiac macrophages (Fig. 6I; Pinto et al., 2012), whereas robust Lyve-1 immunostaining persists in the ventricular endocardium of *H2CKOs* (Fig. 6J, L). However, while Lyve-1 still robustly marks *H2CKO* ventricular endocardium (Fig. 6N white arrow), Lyve-1 expression does not mark the expanded coronary endothelium of *H2CKOs* (Fig. 6N yellow arrow).

As previously mentioned, qPCR demonstrates differential expression of several Vegf signaling components. We therefore investigated, using ChIP, ChIP-seq, EMSA, and luciferase reporter assays, the possibility that Hand2 directly regulates at least a subset of these components (Fig. 7A). Given that our results establish Hand2 as a downstream effector of Notch signaling, and Notch also regulates expression of *VegfRs* within endothelial cells (Herbert and Stainier, 2011), we first addressed the possibility that Hand2 directly regulates *VegfR3* expression. Using the previously described HeLa ChIP samples, we show that

immunoprecipitation of *Hand2-Myc/E12* transfected cell lysates results in selective enrichment of a region within the *VegfR3* promoter that has been previously reported to have regulatory activity (Fig. 7B; Shawber et al., 2007). Furthermore, by EMSA we show that Hand2 E12 heterodimers specifically bind an oligo corresponding to one of the two E-boxes within this human promoter region (Fig. 7C), which consists of the 500bp upstream of the *VegfR3* translation start site. Finally, a luciferase reporter containing the homologous 500bp mouse promoter, was significantly repressed by Hand2 E12 heterodimers (~ 50% repression; $p \leq 0.05$; Fig. 7D). Collectively these data indicate that Hand2 may directly repress *VegfR3* expression within cardiac endothelium.

To detect additional Hand2 targets we utilized a Hand2 ChIP-seq data set that was generated for an alternate study (Osterwalder et al., Dev Cell, in press). This ChIP-seq data set employed a *Hand2-3xFLAG* knock-in allele. E10.5 Hand2 expressing tissues, including the heart, were collected and used for an immunoprecipitation of Hand2-bound regions of genomic DNA. This data set was cross referenced with our *H2CKO* gene expression data, where in addition to increased *VegfR3*, we observed decreased expression of the VegfR2 co-factor *Nrp1*. Analysis of *Hand2-3xFLAG* ChIP-seq data revealed a region of high enrichment 356kb upstream of the *Nrp1* coding region (Fig. 7E and Table S4). An approximately 3kb region containing this potential enhancer was cloned upstream of a luciferase reporter driven by the thymidine kinase (TK) minimal promoter. When co-transfected into HeLa cells with *Hand2* and *E12*, a significant 5.2 fold *trans*-activation was observed (Fig. 7F). Analysis of *VegfR3* and *Nrp1* expression by ISH reveals expression within cardiac endothelium (Fig. S5A, B) although differential expression between controls and *H2CKOs* is not detectable by this non-quantitative assay.

Given that *VegfA* is upregulated by over 200% in E13.5 *H2CKOs*, we analyzed the *Hand2-3xFLAG* ChIP-seq data-set for evidence of direct regulation. No prominent peaks were detected within the *VegfA* locus. Indeed, ISH demonstrates that *VegfA* expression is not detectable within endocardium. However, *VegfA* is strongly expressed within the myocardial compact zone, with low levels of expression observed within trabeculae (Fig. 7G). In *H2CKOs*, the difference in expression levels between compact and trabecular myocardium is visibly less distinct, with high *VegfA* expressing regions appearing to extend beyond the compact zone (Fig. 7H).

Discussion

Loss of *Hand2* within the SHF cardiac progenitors that give rise to both endocardial and myocardial lineages has been associated with TA. In this study, we show that loss of *Hand2* specifically in the endocardium, a cell population in which robust *Hand2* expression has previously gone uninvestigated, can cell autonomously generate TA. These results underscore the importance of effective endocardial-myocardial signaling during early cardiac morphogenesis. Mechanistically, our data show that endocardial Hand2 sits downstream of Notch1 and EfnB2, and is itself directly upstream of *Nrg1*, being necessary and sufficient for *Nrg1* expression *in vivo*. Notch signaling is a well-established component of endocardium-to-myocardium communication. Hand2 endocardial roles include regulation of trabeculation, positioning of the IVS, and IVS morphogenesis. Indeed, endocardial

H2CKOs present multiple septums that are marked by *Irx2* and compact zone/septal marker *Hey2*, while excluding trabecular marker *Anf* (Fig. S2). These ectopic right-sided septa do not express *Hand1* or *Tbx5* at their left side base (Fig. S2I–L), suggesting that these septa form via a non-canonical mechanism from RV cardiomyocytes.

These data demonstrate that endocardial Hand2 regulates the specification of trabecular and septal myocardium from primitive myocardium. Given the striking similarities between the cardiac defects of *EfnB2* knockouts (Fig. 3F, G), which do not express *Nrg1*, and the reported phenotypes of *Nrg1* knockouts (Kramer et al., 1996), the most logical conclusion is that loss of *Nrg1* expression is the root cause of the hypotrabeculation, septal, and TA phenotypes observed in *H2CKOs*.

We show that trabeculation and *Nrg1* expression within *EfnB2* CKO mice is improved by *Hand2* replacement via the *CC-H2* transgene (Fig. 5). Hand2 is necessary for normal expression of *Nrg1* (Fig. 2), and we demonstrate that Hand2 is sufficient for partial restoration of *Nrg1* expression levels in *EfnB2 CKOs*. While trabeculation is markedly improved in *CC-H2*(+) *EfnB2 CKOs*, these embryos still display hallmarks of cardiovascular failure such as pericardial edema and hemorrhage. The incomplete restoration of normal cardiac phenotype is not surprising given that restoration of *Nrg1* expression is incomplete, and EfnB2 signaling likely has a much broader range of endocardial downstream targets then just *Hand2*. Our observation that approximately 37% of *Nrg1* expression remains in *Tie2-Cre H2CKOs* (Fig. 2K) while less than 10% remains in *Tie2-Cre EfnB2 CKOs* (Fig. 3G) indicates that EfnB2 also influences *Nrg1* expression via Hand2-independent inputs.

While it is clear that endocardial loss of *Hand2* impairs the Notch-dependent processes of trabeculation and septal development, it is less clear how this impairment results in TA. It is possible that multiple morphogenic inputs contribute to the TA observed in *H2CKOs*. Previous studies have concluded that TA occurs when the atrial connection to the AV canal expands rightward, but the ventricular inner curvature fails to remodel (Kim et al., 2001). Given the dramatic myocardial defects observed in *H2CKOs*, Hand2-dependent remodeling of AV canal myocardium could be involved; however, histological analysis of *H2CKOs* suggests a simpler model wherein the septum shifts rightward in *H2CKOs* and interferes with development of the primitive right AV canal, thus resulting in TA. Indeed, we show that *Tie2-Cre H2CKOs* have a smaller RV, which is not due to increased cell death within SHF progenitors, increased cell death within the RV, or decreased proliferation within the RV (Fig. S6A–D). Furthermore, analysis of ventricle areas reveals that *Tie2-Cre H2CKOs* have a smaller RV, larger LV, but no change in total area (Fig. S6E), thus supporting histological observations of a rightward shifted septum. In extreme rightward septal shifts, AV cushion maturation is not hindered but the tricuspid valve forms above the LV, thus resulting in DILV. Finally, *Hand2* ablation within the developing OFT and AV valve mesenchyme does not alter septation or valve morphogenesis, and does not result in TA (VanDusen et al., 2014). In total, these data demonstrate a novel cell-autonomous Hand2-dependent role of the endocardium in the etiology of TA/DILV.

In addition to the dramatic defects in myocardial morphogenesis observed in endocardial *H2CKOs*, histological analyses at E13.5 also reveal significant vascular phenotypes.

H2CKOs display precocious and disorganized development of the coronary vascular plexus. Analysis of vascular related gene expression in E10.5 and E13.5 *H2CKOs* surprisingly reveals that major components of cardiac Vegf signaling are dysregulated. *VegfR2* and *VegfD* are downregulated at E10.5, while *VegfR3* and *VegfA* are significantly upregulated by E13.5. Additionally, VegfR2 co-receptor *Nrp1* is downregulated at both E10.5 and E13.5, while expression of the notch ligand *Dll4* is increased at E13.5 – an indication of enhanced Vegf signaling (Fig. 6E, F). Furthermore, qPCR and immunostaining reveals elevated expression of the receptor Lyve-1 within endocardium of E13.5 *H2CKOs*. Analysis at E10.5 demonstrates that Lyve-1 is initially expressed throughout the early endocardium, and is subsequently down-regulated as the endocardium matures, such that by E13.5 expression is no longer detectable within ventricular endocardium, but is observed only within cardiac macrophages. Given the early endocardial expression of Lyve-1, this persistence within *H2CKOs* most likely represents a defect in endocardial maturation, rather than ectopic activation of the lymphatic gene program.

Of the genes we observed to be differentially expressed in E13.5 *H2CKOs*, both the *Dll4* and *Nrp1* loci contain prominent Hand2 Chip-Seq peaks (Table S4). *Nrp1* encodes an isoform-specific VegfA receptor that acts in concert with VegfR2. Interestingly, an RNA subtractive hybridization screen previously identified *Nrp1* as being downregulated in Hand2 systemic null embryos (Yamagishi et al., 2000). Our data indicate that *Nrp1* is an endocardial target of Hand2, although regulation may also occur in additional tissues where these factors are co-expressed (Fig. S5A). Co-transfection of *Hand2* and *E12* with a luciferase reporter containing the potential upstream enhancer region yielded over 5 fold *trans*-activation, further supporting direct regulation of *Nrp1* by Hand2. In contrast, luciferase reporter assays failed to demonstrate Hand2 mediated repression via the enriched Dll4 upstream region, indicating that the increased Dll4 expression in *H2CKOs* may be secondary to changes in expression of Vegf receptors, which are known to regulate Dll4 (Wythe et al., 2013). However, our data do not rule out Hand2 direct regulation of *Dll4* by alternate undetected enhancers. Expression of *VegfR3* is upregulated in E13.5 *H2CKOs* by over 100%. VegfR3 is capable of functioning as both a homo-dimer and VegfR3–VegfR2 hetero-dimer, and distinct functions have been associated with different interactions (Dixelius et al., 2003). VegfR3 plays crucial roles in angiogenic sprouting and development of the lymphatic system (Benedito et al., 2012), and we show that *VegfR3* is expressed within at least a subset of the endocardium (Fig. S5B arrow). While no high-ranking ChIP-Seq peaks were observed within the *VegfR3* locus, cardiac endothelium represents only a small portion of the total *Hand2* expressing tissue that was utilized, and so sensitivity may be a limiting factor of this assay. Our HeLa ChIP results indicate that Hand2 interacts with the *VegfR3* promoter, while transactivation assays correlate with *H2CKO* expression data, indicating that Hand2 may repress *VegfR3* transcription. In addition to *VegfR3*, we observe a 45% increase in *Sox18* expression at E13.5. As *Sox18* specifically marks endothelium of the coronary vasculature at this time-point (Fig. S5C), this increase most likely reflects the hyper-vascularization phenotype.

Similar to several extracardiac angiogenic models of Notch signaling obstruction (Benedito et al., 2012; Tammela et al., 2008), we show that endocardial *Hand2* ablation results in a

hyper-vascularization phenotype featuring the formation of an excessive number of new vessels. Furthermore, we show that this phenotype is accompanied by broad dysregulation of Vegf signaling. Homeostasis of Vegf signaling is crucial during embryonic development, as mice heterozygous for a *VegfA* null mutation die at E9.5, while an increase in *VegfA* expression (~3 fold) results in lethality at approximately E13.5 (Miquerol et al., 2000). In the present study we demonstrate that expression of *VegfA* is expanded in *H2CKOs*. This could reflect aberrant specification of trabecular myocardium, or secondary pathological effects of compromised cardiac function. *VegfA* is the most differentially regulated gene that we observe, while *VegfR2*, *VegfR3*, and *Nrp1* are also dysregulated within *H2CKOs*. Given the complex interactions that take place between these molecules, disrupted receptor stoichiometry and upregulated *VegfA*, a growth factor that is well known for its pro-angiogenic qualities, most likely accounts for the observed coronary phenotype. These data not only provide insight into a second novel function of Hand2 within the endocardium, but also reveal a wider role of Notch signaling during coronary vessel development. Coronary heart disease is a major cause of mortality in developed nations, being responsible for approximately one of every six deaths in the United States (Go et al., 2013). Consequently, further assessment of Hand2's regulatory role in Vegf signaling during coronary vascularization, as well as potential adult homeostatic roles of Hand2-dependent Notch signaling, are interesting avenues of future investigations.

Experimental Procedures

Mice and Genotyping

Tie2-Cre(+) and *Nfatc1-Cre(+)* mice were crossed with *Hand2*$^{+/-}$ mice to generate *Tie2-Cre(+);Hand2*$^{+/-}$ and *Nfatc1-Cre(+);Hand2*$^{+/-}$ males. These males were then crossed with *Hand2*$^{fx/fx}$*;ROSA26R* reporter mice (*lacZ* or *eYFP*) to generate conditional null *Hand2* embryos. *Tie2-Cre(+)* females were crossed with *EfnB2*$^{fx/fx}$ males to generate *Tie2-Cre(+);EfnB2*$^{fx/+}$ males. These males were then crossed with *EfnB2*$^{fx/fx}$ females to generate conditional null *EfnB2* embryos. The cre-activatable transgene *CAG-CAT-Hand2* was constructed by replacing the *Myc-Twist1* cDNA of *CAG-CAT-Twist* (Connerney et al., 2006) with the murine *Myc-Hand2* cDNA. This construct was used for microinjection to establish a transgenic line. For genotyping information see Supplemental Procedures. Mouse maintenance and experimentation was performed according to protocols approved by the IUSOM IACUC.

Hand2-3xFLAG ChIP-Seq

The Hand2 ChIP-Seq dataset was generated as part of a previous study using homozygous *Hand2-3xFLAG* embryos, which express a 3xFLAG epitope-tagged Hand2 protein (Osterwalder et al., Dev Cell, submitted). Briefly, Hand2 expressing tissues (heart, limbs and pharyngeal arches) from 150 *Hand2-3xFLAG* E10.5 embryos were dissected and pooled. Samples were cross-linked in 1% formaldehyde for 5 minutes and ChIP was performed using FLAG antibodies (Sigma F1804). ChIP-Seq reads were mapped to the mouse genome (NCBI37/mm9) and peaks were detected using MACS (version 1.3.7.1) for the *HAND2-3xFLAG* and input control samples. Statistically validated peaks were sorted according to fold-enrichment and number of reads.

Section RNA *In Situ* Hybridization

Antisense digoxygenin labeled riboprobes were transcribed with T7, SP6, or T3 (Roche). Section *In Situ* hybridization was performed as previously described (Vincentz et al., 2008). The cDNA for a *Fog2* ribo-probe was kindly supplied by Eric Svensson, *Tbx20* by Simon Conway, *Anf* and *Irx2* by Vincent Christoffels, *TgfβR2* from Henry Sucov, and *EfnB2* from Hai Wang. All data reflect assessment in n≥3 embryos for *ISH*, and immunostaining, and n≥4 for qRT-PCR analyses.

Quantitative RT-PCR

Total RNA was isolated from E10.5 or E13.5 ventricles using the High Pure RNA Isolation Kit (Roche). This RNA served as a template to generate cDNA using the Transcriptor First Strand cDNA Synthesis Kit (Roche). For qPCR, cDNA was amplified using Taqman Probe-Based Gene Expression Assays (Applied Biosystems). Relative gene expression was determined after normalization to GAPDH. The Student's t-test was used to detect significant differences between sample groups; asterisks denotes p-values ≤ 0.05. Error bars represent standard error (SE).

EMSAs, luciferase assays and ChIP

Hand2 and E12 were *in vitro* translated using the Promega Reticulocyte Lysate System. 5ul of translated protein was incubated with radio-labeled oligos corresponding to E-boxes and D-boxes within the *Nrg1* and *VegfR3* loci, in binding buffer for 30 minutes at 25°C (Firulli et al., 2007). Transcription factor/oligo complexes were run out on a non-denaturing 6% polyacrylamide gel and assessed on a phospho-imager. For luciferase assays, HeLa cells were transfected using X-tremeGENE HP (Roche) at a ratio of 3:1 with *Nrg1-500bp +pGL4.10* (luciferase), *VegfR3-500bp+pGL4.10* (luciferase), *pGL4.73* (SV40-renilla) or *pGL4.74* (TK-renilla), *Pcs2+Myc-Hand2*, *Pcs2+Myc-E12*, *pcDNA+Myc-ΔBasic-Hand2* (kindly provided by Eric Olson), or *pcDNA3.1*, and cultured for 48 hours. After harvest and processing, luciferase and renilla reporter activity was assessed in equal amounts of cell lysate using Luminoskan Ascent software and a ThermoLabsystems luminometer. Luciferase results were normalized to protein concentration or renilla. Asterisks denote significant difference from *pcDNA* control (pvalue≤0.05); error bars represent SE. For construction of Nrp1(−358/−355kb) and Dll4(−23/−20kb) luciferase reporters, genomic regions containing a *Hand2-3xFLAG* ChIP-Seq peak were PCR amplified and cloned into *TK-pGL4.10*. For chromatin immunoprecipitation (ChIP) of the *Nrg1* promoter, HeLA cells were again transfected using X-tremeGENE HP at a ratio of 3:1. After culturing for 48 hours, cells were processed as previously described (Barnes et al., 2011). Briefly, equal amounts of sheered chromatin were immunoprecipitated overnight at 4°C with 50ul of αMyc-conjugated agarose beads (Sigma), or beads without antibody for a negative control. After reversing crosslinks, eluted immunoprecipitated DNA was phenol chloroform extracted, resuspended in ddH_2O, and used for subsequent PCR reactions. After 37 cycles of PCR amplification, product was analyzed on an agarose gel. ChIP transfection constructs included *Pcs2+Myc-Hand2*, *Pcs2+E12*, and *Pcs2+Myc*. See supplemental procedures for oligo information.

Supplementary Material

Refer to Web version on PubMed Central for supplementary material.

Acknowledgements

We thank Danny Carney and Hannah Lohr for technical assistance and support. We also thank the Riley Heart Research Center Group for discussion and helpful feedback. Furthermore, we thank Thomas Coate for kindly providing *EfnB2*$^{fx/fx}$ mice. Infrastructural support at the Herman B Wells Center is partially supported by the Riley Children's Foundation and the Carleton Buehl McCulloch Chair. Grant support for this work was provided by NIH 1R01HL120920-01, 1R01HL122123-01, and 1R0AR061392-03 (ABF) and American Heart Association predoctoral fellowship 12PRE11700006 (NJV).

References

Anderson R, Becker A, Macartney F, Shinebourne E, Wilkinson J, Tynan M. Is “tricuspid atresia” a univentricular heart? Pediatric Cardiology. 1979; 1:51–56.

Barnes RM, Firulli BA, VanDusen NJ, Morikawa Y, Conway SJ, Cserjesi P, Vincentz JW, Firulli AB. Hand2 Loss-of-Function in Hand1-Expressing Cells Reveals Distinct Roles in Epicardial and Coronary Vessel Development. Circulation Research. 2011; 108:940–949. [PubMed: 21350214]

Benedito R, Rocha SF, Woeste M, Zamykal M, Radtke F, Casanovas O, Duarte A, Pytowski B, Adams RH. Notch-dependent VEGFR3 upregulation allows angiogenesis without VEGF-VEGFR2 signalling. Nature. 2012; 484:110–114. [PubMed: 22426001]

Chen H, Shi S, Acosta L, Li W, Lu J, Bao S, Chen Z, Yang Z, Schneider MD, Chien KR, et al. BMP10 is essential for maintaining cardiac growth during murine cardiogenesis. Development. 2004; 131:2219–2231. [PubMed: 15073151]

Connerney J, Andreeva V, Leshem Y, Muentener C, Mercado MA, Spicer DB. Twist1 dimer selection regulates cranial suture patterning and fusion. Dev Dyn. 2006; 235:1345–1357. [PubMed: 16502419]

Dixelius J, Mäkinen T, Wirzenius M, Karkkainen MJ, Wernstedt C, Alitalo K, Claesson-Welsh L. Ligand-induced vascular endothelial growth factor receptor-3 (VEGFR-3) heterodimerization with VEGFR-2 in primary lymphatic endothelial cells regulates tyrosine phosphorylation sites. Journal of Biological Chemistry. 2003; 278:40973–40979. [PubMed: 12881528]

Ferrara, N.; Carver Moore, K.; Chen, H.; Dowd, M.; Lu, L.; O'Shea, KS.; Powell Braxton, L.; Hillan, KJ.; Moore, MW. Heterozygous embryonic lethality induced by targeted inactivation of the VEGF gene. 1996.

Firulli BA, Redick BA, Conway SJ, Firulli AB. Mutations within helix I of Twist1 result in distinct limb defects and variation of DNA binding affinities. J Biol Chem. 2007; 282:27536–27546. [PubMed: 17652084]

Frensing T, Kaltschmidt C, Schmitt-John T. Characterization of a neuregulin-1 gene promoter: positive regulation of type I isoforms by NF-kappaB. Biochim Biophys Acta. 2008; 1779:139–144. [PubMed: 18082154]

Gerety SS, Anderson DJ. Cardiovascular ephrinB2 function is essential for embryonic angiogenesis. Development. 2002; 129:1397–1410. [PubMed: 11880349]

Go AS, Mozaffarian D, Roger VL, Benjamin EJ, Berry JD, Borden WB, Bravata DM, Dai S, Ford ES, Fox CS, et al. Heart disease and stroke statistics--2013 update: a report from the American Heart Association. Circulation. 2013; 127:e6–e245. [PubMed: 23239837]

Grego-Bessa J, Luna-Zurita L, del Monte G, Bolos V, Melgar P, Arandilla A, Garratt AN, Zang H, Mukouyama YS, Chen H, et al. Notch signaling is essential for ventricular chamber development. Dev Cell. 2007; 12:415–429. [PubMed: 17336907]

Herbert SP, Stainier DY. Molecular control of endothelial cell behaviour during blood vessel morphogenesis. Nat Rev Mol Cell Biol. 2011; 12:551–564. [PubMed: 21860391]

Hoffman JI. Incidence of congenital heart disease: I. Postnatal incidence. Pediatr Cardiol. 1995; 16:103–113. [PubMed: 7617503]

Jiao K, Langworthy M, Batts L, Brown CB, Moses HL, Baldwin HS. Tgfbeta signaling is required for atrioventricular cushion mesenchyme remodeling during in vivo cardiac development. Development. 2006; 133:4585–4593. [PubMed: 17050629]

Kim JS, Viragh S, Moorman AF, Anderson RH, Lamers WH. Development of the myocardium of the atrioventricular canal and the vestibular spine in the human heart. Circ Res. 2001; 88:395–402. [PubMed: 11230106]

Kisanuki YY, Hammer RE, Miyazaki J, Williams SC, Richardson JA, Yanagisawa M. Tie2-Cre transgenic mice: a new model for endothelial cell-lineage analysis in vivo. Dev Biol. 2001; 230:230–242. [PubMed: 11161575]

Kramer R, Bucay N, Kane DJ, Martin LE, Tarpley JE, Theill LE. Neuregulins with an Ig-like domain are essential for mouse myocardial and neuronal development. Proceedings of the National Academy of Sciences. 1996; 93:4833–4838.

McFadden DG, McAnally J, Richardson JA, Charité J, Olson EN. Misexpression of dHAND induces ectopic digits in the developing limb bud in the absence of direct DNA binding. Development. 2002; 129:3077–3088. [PubMed: 12070084]

Miquerol L, Langille BL, Nagy A. Embryonic development is disrupted by modest increases in vascular endothelial growth factor gene expression. Development. 2000; 127:3941–3946. [PubMed: 10952892]

Pinto AR, Paolicelli R, Salimova E, Gospocic J, Slonimsky E, Bilbao-Cortes D, Godwin JW, Rosenthal NA. An abundant tissue macrophage population in the adult murine heart with a distinct alternatively-activated macrophage profile. PloS one. 2012; 7:e36814. [PubMed: 22590615]

Red-Horse K, Ueno H, Weissman IL, Krasnow MA. Coronary arteries form by developmental reprogramming of venous cells. Nature. 2010; 464:549–553. [PubMed: 20336138]

Shawber CJ, Funahashi Y, Francisco E, Vorontchikhina M, Kitamura Y, Stowell SA, Borisenko V, Feirt N, Podgrabinska S, Shiraishi K, et al. Notch alters VEGF responsiveness in human and murine endothelial cells by direct regulation of VEGFR-3 expression. J Clin Invest. 2007; 117:3369–3382. [PubMed: 17948123]

Smart N, Dubé KN, Riley PR. Coronary vessel development and insight towards neovascular therapy. International journal of experimental pathology. 2009; 90:262–283. [PubMed: 19563610]

Svensson EC, Huggins GS, Lin H, Clendenin C, Jiang F, Tufts R, Dardik FB, Leiden JM. A syndrome of tricuspid atresia in mice with a targeted mutation of the gene encoding Fog-2. Nat Genet. 2000; 25:353–356. [PubMed: 10888889]

Takeuchi JK, Ohgi M, Koshiba-Takeuchi K, Shiratori H, Sakaki I, Ogura K, Saijoh Y, Ogura T. Tbx5 specifies the left/right ventricles and ventricular septum position during cardiogenesis. Development. 2003; 130:5953–5964. [PubMed: 14573514]

Tammela T, Zarkada G, Wallgard E, Murtomaki A, Suchting S, Wirzenius M, Waltari M, Hellstrom M, Schomber T, Peltonen R, et al. Blocking VEGFR-3 suppresses angiogenic sprouting and vascular network formation. Nature. 2008; 454:656–660. [PubMed: 18594512]

Tian X, Hu T, Zhang H, He L, Huang X, Liu Q, Yu W, Yang Z, Zhang Z, Zhong TP, et al. Subepicardial endothelial cells invade the embryonic ventricle wall to form coronary arteries. Cell Res. 2013; 23:1075–1090. [PubMed: 23797856]

Tsuchihashi T, Maeda J, Shin CH, Ivey KN, Black BL, Olson EN, Yamagishi H, Srivastava D. Hand2 function in second heart field progenitors is essential for cardiogenesis. Dev Biol. 2011; 351:62–69. [PubMed: 21185281]

VanDusen NJ, Vincentz JW, Firulli BA, Howard MJ, Rubart M, Firulli AB. Loss of Hand2 in a population of Periostin lineage cells results in pronounced bradycardia and neonatal death. Developmental biology. 2014; 388:149–158. [PubMed: 24565998]

Verzi MP, McCulley DJ, De Val S, Dodou E, Black BL. The right ventricle, outflow tract, and ventricular septum comprise a restricted expression domain within the secondary/anterior heart field. Developmental Biology. 2005; 287:134–145. [PubMed: 16188249]

Vincentz JW, Barnes RM, Rodgers R, Firulli BA, Conway SJ, Firulli AB. An absence of Twist1 results in aberrant cardiac neural crest morphogenesis. Dev Biol. 2008; 320:131–139. [PubMed: 18539270]

Wu B, Zhang Z, Lui W, Chen X, Wang Y, Chamberlain AA, Moreno-Rodriguez RA, Markwald RR, O'Rourke BP, Sharp DJ, et al. Endocardial cells form the coronary arteries by angiogenesis through myocardial-endocardial VEGF signaling. Cell. 2012; 151:1083–1096. [PubMed: 23178125]

Wythe JD, Dang LT, Devine WP, Boudreau E, Artap ST, He D, Schachterle W, Stainier DY, Oettgen P, Black BL, et al. ETS Factors Regulate Vegf-Dependent Arterial Specification. Dev Cell. 2013; 26:45–58. [PubMed: 23830865]

Yamagishi H, Olson EN, Srivastava D. The basic helix-loop-helix transcription factor, dHAND, is required for vascular development. J Clin Invest. 2000; 105:261–270. [PubMed: 10675351]

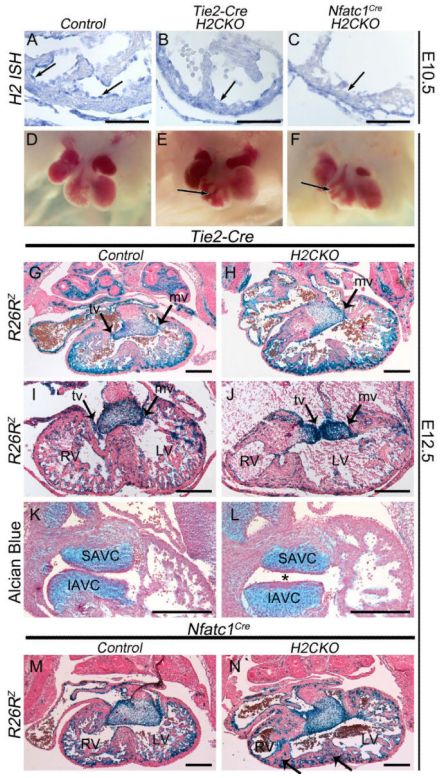

Figure 1. Endocardial deletion of *Hand2* results in a VSD, hypotrabeculation, hypoplastic RV, IVS defects and TA

Hand2 ISH of RV section from E10.5 control, *Tie2-Cre H2CKO*, and *Nfatc1*^{Cre}*H2CKO*, respectively (A–C). Wholemount view of E12.5 control heart, *Tie2-Cre H2CKO*, and *Nfatc1*^{Cre} *H2CKO*, respectively (D–F). *R26R*^{lacZ} stained sections from E12.5 *Tie2-Cre*(+) control embryo (G), *Tie2-Cre H2CKO* with TA (H). *R26R*^{lacZ} stained E12.5 *Tie2-Cre*(+) control embryo (I), and *Tie2-Cre H2CKO* with DILV (J). *R26R*^{lacZ} stained sections from E12.5 *Nfatc1*^{Cre} control embryo (M), and *Nfatc1*^{Cre} *H2CKO* (N; arrows denote multiple IVSs). Alcian blue staining of E12.5 *Tie2-Cre*(+) control AV cushions (K), and *Tie2-Cre H2CKO* (L). Asterisk denotes abnormalities in AV cushion shape and position. SAVC, superior atrioventricular cushion; IAVC, inferior atrioventricular cushion; tv, tricuspid valve; mv, mitral valve. Scale bars in A – C represent 100μm; scale bars in G – N represent 250μm.

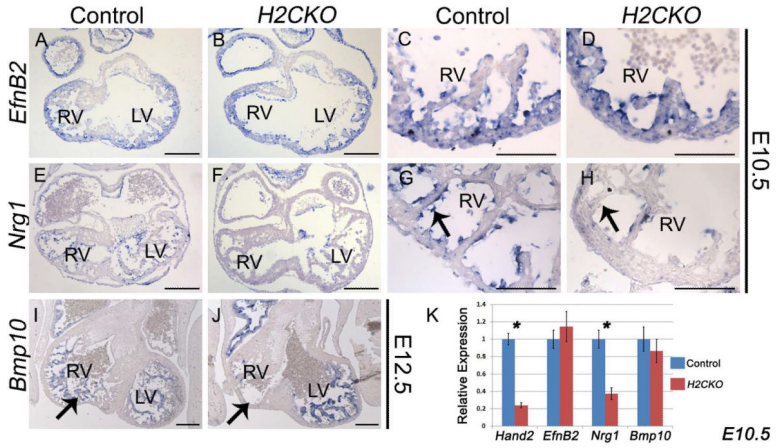

Figure 2. *H2CKOs* exhibit down-regulation of *Nrg1*, and loss of *Bmp10* expressing trabecular myocardium

Expression of the Notch1 target *EfnB2* is comparable between *H2CKOs* at E10.5 with controls (A–D). *Nrg1* expression at E10.5 is markedly decreased in *H2CKOs* when compared to controls (E–H arrows in G and H denote endocardium). *H2CKOs* have less *Bmp10* expressing trabecular myocardium in the RV at E12.5 (I, J arrows denote trabecular tissue). qPCR on isolated ventricles confirms the significant reduction (* p≤0.05) of *Nrg1* in E10.5 *H2CKOs*. Scale bars in A, B, E, F, I, and J represent 200μm; scale bars in C, D, G, and H represent 100μm.

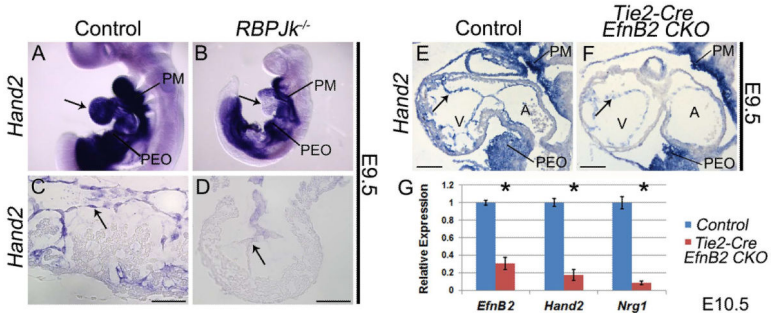

Figure 3. Hand2 functions downstream of Notch1 and the direct Notch1 target EphrinB2 during trabeculation

Wholemount *Hand2* ISH in wild type (A) and *RBPJk* knockout embryos (B). Arrows indicate endocardial *Hand2* expression in control (A) and loss of expression in *RBPJk* knockouts (B). *Hand2* ISH (C) shows robust endocardial Hand2 expression that is downregulated within RBPJk$^{-/-}$ endocardium (D). *Hand2* ISH (E) revealed a similar downregulation of *Hand2* within the endocardium of *Tie2-Cre EfnB2CKO* hearts (F Arrows denote endocardium). PM, pharyngeal mesenchyme; PEO, proepicardial organ. qPCR on RNA isolated from ventricles confirms significant (* p≤0.05) downregulation of *Hand2* and *Nrg1* in *Tie2-Cre EfnB2CKO* hearts (G). Scale bars in C and D represent 50μm; scale bars in E and F represent 100μm.

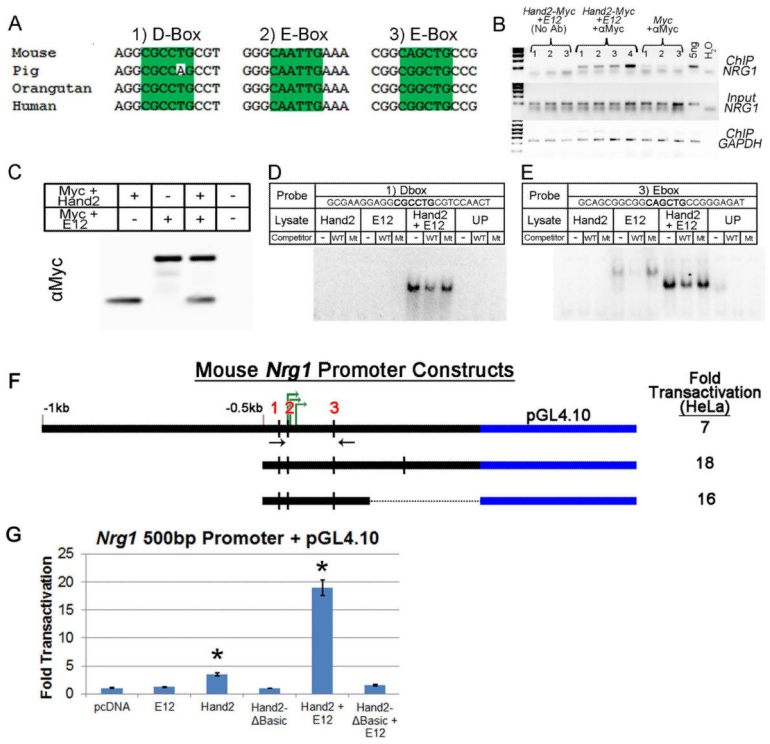

Figure 4. Hand2 directly regulates *Nrg1*

Sequence alignments reveal three Hand2 consensus sites that are highly conserved among mammals (A). ChIP of the *NRG1* promoter (B). *In-vitro* transcribed and translated Hand2 and E12 used in EMSAs (C). EMSAs for D-box 1 (D) and E-box 3 (E) show robust and specific binding of Hand2-E12 heterodimers. No binding is observed for site 2. Luciferase reporter assays with a deletion series of the *Nrg1* promoter. Red numbers denote positions of the Hand2 consensus sites; green arrows denote positions of the transcription start sites; black arrows, location of ChIP primers (F). Transactivation of 500bp *Nrg1* promoter reporter (G; *p≤0.05).

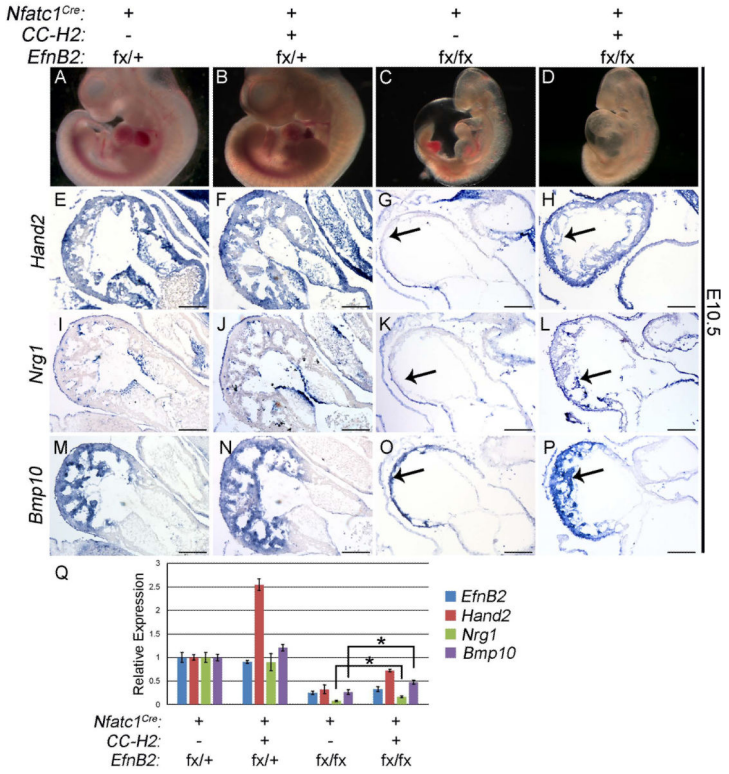

Figure 5. Conditional *CAG-CAT-Hand2* transgene expression in *Nfatc1*^{Cre} *EfnB2 CKOs* partially improves trabeculation and *Nrg1* expression

Wholemount images of E10.5 control, *CC-H2(+)* control, *EfnB2 CKO*, and *CC-H2(+)*; *EfnB2 CKO* embryos (A–D). *Hand2* section ISH (E–H). Arrow in G indicates loss of *Hand2*; arrow in H indicates restoration of endocardial Hand2 via *CC-H2*. *Nrg1* section ISH (I–L). Arrow in K indicates loss of *Nrg1 in EfnB2 CKOs*; arrow in L indicates restored *Nrg1* expression in *EfnB2 CKOs* that are also *CC-H2(+).Bmp10* section ISH (M–P). Arrow in O indicates *Bmp10* expressing myocardium and lack of trabeculation; arrow in P indicates restoration of *Bmp10* expressing trabeculations. qPCR analysis of isolated E10.5 ventricles (Q). Asterisks denote significant difference ($p \leq 0.05$). *CC-H2*, *CAG-CAT-Hand2*. Scale bars in E – P represent 100μm.

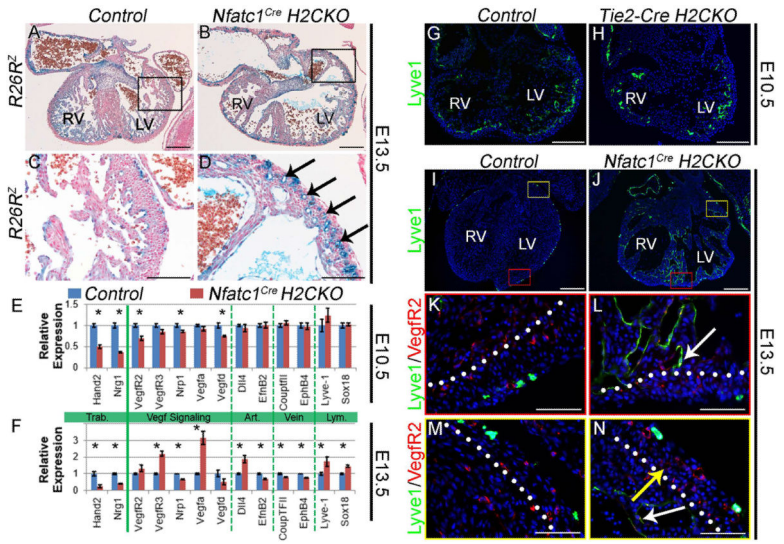

Figure 6. Hand2 controls coronary development and endocardial maturation via regulation of Vegf signaling

R26R^{lacZ} stained E13.5 hearts (A, B). LV outer curvature (C, D). *Nfatc1*^{Cre} *H2CKOs* display hyper-vascularization (arrows in D). qPCR analysis of E10.5 and E13.5 gene expression (n = 4) in *Nfatc1*^{Cre} *H2CKOs* (E, F; Asterisks denote significant difference ($p \leq 0.05$). Lyve-1 immunostaining in E10.5 Control and *Tie2-CreH2CKO* hearts (G, H). Lyve-1 immunostaining in E13.5 Control and *Nfatc1*^{Cre} *H2CKO* hearts (I–N). In E13.5 control hearts Lyve-1 expression is restricted to endothelial lymphatic precursors (K), while *H2CKOs* continue to express Lvye-1 within ventricular endocardium (L white arrow). Persistent Lyve-1 expression marks ventricular endocardium (N white arrow) but not coronary endothelium (N yellow arrow). Dotted lines denote the border between compact and trabecular myocardium. Scale bars in A and B represent 250μm, 100μm for C and D, 200μm for G and H, 250μm for I and J, and 50μm for K–N.

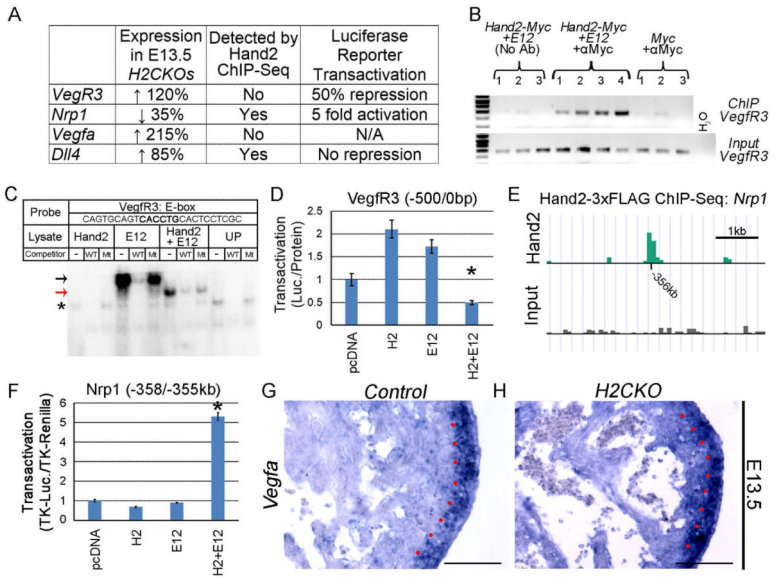

Figure 7. Hand2 regulates Vegf signaling

Differentially expressed genes that were analyzed for direct regulation by Hand2 (A). ChIP of a region within the 500bp *VegfR3* promoter (B). EMSA demonstrates Hand2-E12 heterodimers specifically bind an oligo corresponding to an E-box within the ChIP amplicon of the *VegfR3* promoter (C). Black arrow indicates E12 homodimer binding, red arrow indicates Hand2-E12 heterodimer binding, and asterisk indicates nonspecific binding. Hand2-E12 heterodimers repress significantly ($p \leq 0.05$) a luciferase reporter containing the 500bp *VegfR3* promoter (D). *Hand2-3xFLAG* ChIP-seq demonstrates a prominent region of enrichment approximately 356kb upstream of the *Nrp1* coding region (E). A luciferase reporter containing this potential enhancer region is significantly ($p \leq 0.05$) *trans*-activated 5-fold by H2-E12 heterodimers (F). ISH demonstrates strong myocardial expression of *VegfA* within the compact zone of control E13.5 hearts (G). Red dots denote the border between compact and trabecular myocardium. In *H2CKOs*, the distinction between *VegfA* expression levels in compact versus trabecular myocardium is more poorly defined (H). Scale bars in G and H represent 100μm.